N89-13314

Tests of a Multichannel Photometer Based on Silicon Diode Detectors

W.J. Borucki
NASA Ames Research Center, Moffett Field, CA 94035

L.E. Allen, S.W. Taylor, E.B. Torbet
SETI Institute, 101 First Street, #410, Los Altos, CA 94022

A.R. Schaefer, J. Fowler
National Bureau of Standards, Gaithersburg, MD 20899

ABSTRACT

The photometric method of planetary detection requires the simultaneous monitoring of many stars to a precision near one part in 10^5 for the detection of Earth-sized planets. A breadboard of a three-channel photometer has been constructed and tested. The detectors are silicon photodiodes that have a noise equivalent power of 3×10^{-15} W/$\sqrt{\text{Hz}}$ and internal quantum efficiency near unity. The amplifier unit consists of three identical but independent transimpedance converters that develop 10^{11} volts/amp. Observations of both lab sources and stars have been conducted. Lab tests of the system show hour-to-hour precision of 2×10^4 for the ratios of channel outputs. Field tests of the breadboard at Lick Observatory show that after correction for extinction variations, a scintillation-limited precision is obtained for stellar flux ratios. Tests conducted with the 0.5 m aperture Carnegie Twin Astrograph attained a precision for the ratio of our program stars (α and β ARI) of 1×10^3 (i.e., 1 millimag.) for a 3-minute integration time. Cooling the detectors and amplifiers to cryogenic temperatures will be required to observe stars with $m_v > 4$. Efforts are underway to reduce the internal noise in order to observe fainter stars.

I. INTRODUCTION

The photometric method of detecting planetary systems depends on observing the change in the stellar flux when a planet transits a star (Rosenblatt, 1971, and Borucki and Summers, 1984). The magnitude of the flux change is directly proportional to the ratio of the planet's area to that of the star. A transit of the sun by Jupiter or Saturn would reduce the observed stellar flux by $\sim$ 1%, a transit by Uranus or Neptune by $\sim$ 0.1%, and a transit by Earth or Venus, $\sim$ 0.01%. While the detecton of earth-sized planets will require observations from a space platform to overcome atmospheric effects (Borucki, 1984), the

precision required to detect larger planets can be achieved using ground-based state-of-the-art photometers. Improved instrumentation and careful technique already measure flux changes of 0.3% (Radick et al., 1987).

Since the photometric method of detecting other planetary systems works only for planets that have orbital planes near our line of sight, many stars must be monitored to insure that some stars with appropriately oriented orbital planes are observed. Borucki and Summers (1984) have shown that, if every solar-type star has a planetary system similar to ours, then a photometer with the requisite precision that monitors 1000 stars should detect at least 10 transits per year of observation. A three-year observation program from a space platform would produce a meaningful estimate of the frequency of Earth-sized planets around other stars.

This paper describes tests of a breadboard photometer that uses silicon photodiodes with which we obtained a precision of 2×10^4 .

II. INSTRUMENTATION

A schematic diagram of the photometer is shown in Figure 1. The photometer was constructed with 3 channels so that it could monitor 2 stars and the sky simultaneously. The detectors are PNN^+ – type silicon photodiodes manufactured by Hamamatsu Corp. (S1226 series). These detectors have a Noise Equivalent Power of 3×10^{-15} W/$\sqrt{\text{Hz}}$ at 20° C. Their internal quantum efficiency is near unity: one electron-hole pair is produced for each photon that enters the detector. The properties of this detector type have been studied and documented by Zalewski and Geist (1980), Geist et al. (1982), and Schaefer (1984). Also see the discussion in this volume by Eppeldauer and Schaefer. The photon spectral response is nearly constant in the 500 to 700 nm range. The detectors are mounted in modules that hold the spectral bandpass filters. These modules are placed behind a mask that has been machined to match the star field of interest. The mask with the detector modules is placed in the focal plane of a telescope.

The pre-amplifier system consists of three identical but independent current-to-voltage converters that develop 10^{11} volts/amp and have a 1-second time constant. To reduce temperature differences between pre-amps, the pre-amps were constructed on three printed circuit boards that are mounted in an equalateral triangle configuration inside of a heavy aluminum cyclinder. The pre-amps are sampled by high-precision HP-3457 multimeters that are controlled by an IBM-PC computer via a GPIB bus. This data acquisition computer reads the signal from the multimeters and writes it to a floppy disk. The data on the floppy disk are then transferred to another computer for analysis.

To correct the air mass for changes in atmospheric pressure during the observations, data from a digital barometer with an accuracy of 0.1 millibar are frequently recorded by the data acquisition computer.

III. LABORATORY TESTS

Laboratory tests were conducted to determine the noise characteristics of the photometer. To remove the noise introduced by slow drifts in the dark current, the signal is chopped by alternately opening and closing a shutter. The dark current measurements are then interpolated and subtracted from the measurements made while the shutter is open. The signal integration period is made 10 times as long as the integration period for the dark current because the fluctuations in the stellar signal levels are typically much larger than those of the dark current. Further, a wait period of 10 time constants is used when the shutter is first opened or closed to insure that the circuitry has had time to fully adjust to the new signal level. The measured noise current at room temperature for sixty-second samples is 3×10^{-4} volts measured at the output of the preamps. Because these preamps develop 10^{11} volts/amp, this noise voltage represents a noise current of 3×10^{-15} amps at the detectors. Measurements conducted without detectors show that the observed noise was generated by the preamps rather than by the detectors.

Because of the correlations present in the data, a higher precision is obtained when signal ratios rather than the outputs from individual channels are considered. Define the expected noise n_{12} , as the standard deviation of the ratio of two channel outputs:

$$n_{12} = \text{S.D.}\{V_1/V_2\} \tag{1}$$

where V_i is the signal in channel "i" and S.D. {} refers to the standard deviation of the quantity enclosed in the braces. We define the precision as the reciprocal of the normalized standard deviation:

$$P = \frac{(V_1/V_2)}{\text{S.D.}\{V_1/V_2\}} \tag{2}$$

For equal amplitude signals, and noise that shows no cross correlation, the precision P, should be approximately:

$$P = (\frac{V}{\text{S.D.}\{V\}})/\sqrt{2} \tag{3}$$

However, if the noise is correlated between the channels, then P can be larger than that given by Eq. 3. Although light-source fluctuations are much larger than the dark current noise, all the channels observe the same light source simultaneously. Consequently, no noise is introduced into the ratios by the light source and the dominant noise sources become the dark current and drift in the amplifier gains ("gain drift"). Correlation coefficients of 0.4 and 0.995 were measured for 60-second samples of the dark current and gain drift, respectively. Figure 2 shows the measured precision versus the integration time. Precision reaches approximately 2×10^4 for integration times near 2000 sec. However, at larger integration times, the curve departs from a square root dependence on τ and shows little gain in precision with increasing τ. For such long integration times, very-long-period differential drifts of the amplifiers limit the attainable precision.

IV. FIELD TESTS

Several tests of the photometer were made in the summer and fall of 1986 using the Carnegie Twin Astrograph at Lick Observatory. Presented here are observations of a pair of known non-variable stars: α Aries (K2 III, $m_v = 2.0$) and β Aries (A5 V, $m_v = 2.6$). All three photometer channels used identical filters. The filters transmit from 520 nm to 650 nm, a range similar to the V band of the UBV system. The short wavelength was defined by the Schott GG14 filter permanently installed in the Twin Astrograph and the long wavelength limit was defined by short wave pass filters installed in the detector modules. Because no transformations from the instrument system were contemplated, no transformation coefficients were determined.

At the beginning of each measurement sequence, and after every 10^{th} measurement, the telescope shutter was closed and the dark current was measured in each of the three channels.

To correct for atmospheric extinction we can write the observed flux $I(t)$ as a function of the above-atmosphere flux $I_\circ$ (assumed to be constant), the air mass $x(t)$, and the extinction coefficient per unit air mass $k(t)$:

$$I(t) = I_\circ 10^{-2.5k(t)x(t)} \tag{4}$$

Because differential photometry, rather than absolute photometry will be considered, only the flux ratio of one star to another star or to a group of stars is of interest. For simplicity, consider only two stars 1, and 2, and write their ratio as:

$$\frac{I_{1_\circ}}{I_{2_\circ}} = \frac{I_1(t)}{I_2(t)} 10^{2.5[k_1(t)x_1(t) - k_2(t)x_2(t)]} \tag{5}$$

Even though the two stars are observed simultaneously and are near enough in the sky to be in the same field of view, the values of the air mass are not identical and therefore cannot be factored out of the square bracket. Furthermore, because the stars do not have the same spectrum, the extinction coefficients for the two stars will be different even though identical filters and detectors are used. Although the two products in the square brackets do not cancel, the difference of the products is small enough to greatly reduce the sensitivity of the ratio $I_1(t)/I_2(t)$ to variations in extinction. Figure 3 shows the measured variation of the extinction coefficient during a typical night. This figure shows that the extinction coefficient fell to 1/3 of its original value during the night. Breaks in the curve occur whenever the telescope shutter closes so that the dark currents can be measured.

Without correcting for extinction variations, the ratio of the stellar fluxes varied by only 2%. (See Figure 4) These measurements show, however, that even for relative photometry, it is necessary to measure and correct for the variations in $k(t)$ if a measurement precision of 50 or better is required.

The increased precision that is obtained when measurements of the target star, reference star, and the sky are observed simultaneously is shown in Figure 5. For the data shown in this figure the extinction coefficient of the target star (β Ari) was determined from measurements on the reference star. The symbols represent the precision obtained for

three consecutive nights. The lower solid curve is the scintillation-limited precision for the ratio of two uncorrelated channels. It was calculated by dividing the average of the measured precision of individual channels by $\sqrt{2}$ based on the assumption that the variance of the ratio is equal to the sum of the variances of the individual channels. The measured variances for individual channels are approximately those calculated from Young (1974) for our telescope aperture and integration times. For integration times in excess of 10 sec, the precision of the ratio is typically a factor of 2 greater than that of individual channels. These results indicate that outputs from the channels are weakly correlated. The approximate agreement between the data and the prediction indicates that we have attained scintillation limited precision and no further improvement can be expected unless the telescope aperture is increased, the integration times are increased, or the observations are made during nights when less scintillation is present. The upper curve in Figure 5 represents the precision attained in the laboratory. These values are four to ten times higher then those attained by the telescopic observations. They imply that the precision of the measurements will be limited by the photometer only when the telescope aperture exceeds approximately 3 m.

CONCLUSIONS

A breadboard photometer has been constructed that demonstrates a precision of 2×10^4 in the laboratory and scintillation-limited performance when used with a 0.5 m aperture telescope. Because the detectors and preamps are not cooled, only stars with $m_v \leq 4$ are bright enough to allow the photometer to attain a precision of 1×10^3 for 3-minute observations with a 0.5 m aperture telescope. Cooling the photometer should allow much fainter stars to observed. Increasing the aperture of the telescope will allow higher precision and the observation of fainter stars.

REFERENCES

Borucki, W.J. (1984). Photometric precision needed for planetary detection. Proceedings of the Workshop on Improvements to Photometry, held at San Diego State University, San Diego, CA, June 18–19, 1984. NASA CP 2350.

Borucki, W.J., and A.L. Summers (1984). The photometric method of detecting other planetary systems. Icarus 58, 121–134.

Geist, J., W.K. Gladden, & E.F. Zalewski (1982). Physics of photon-flux measurements with silicon photodiodes. J. Appl. Opt. Soc. Am. 72, 1068–1075.

Radick, R.R., D.T. Thompson, G.W. Lockwood, D.K. Duncan, & W.E. Baggett (1987). The activity, variability, and rotation of lower main-sequence Hyades stars. Ap.J. 321, 459–472.

Rosenblatt, F. (1971). A two-color method for detection of extra- solar planetary systems. Icarus 14, 71–93.

Schaefer, A.R. (1984). Photodiodes for astronomical stellar radiometry. Proceedings of the Workshop on Improvements to Photometry, held at San Diego State University, San Diego, CA, June 18–19, 1984. NASA CP 2350.

Young, A.T. (1974). Observational technique and data reduction. Methods of Experimental Physics, 12A. Edited by N. Carleton.

Zalewski, E.F., and J. Geist (1980). Silicon photodiode absolute spectral response self-calibration. Appl. Optics 19, 1214–1216.

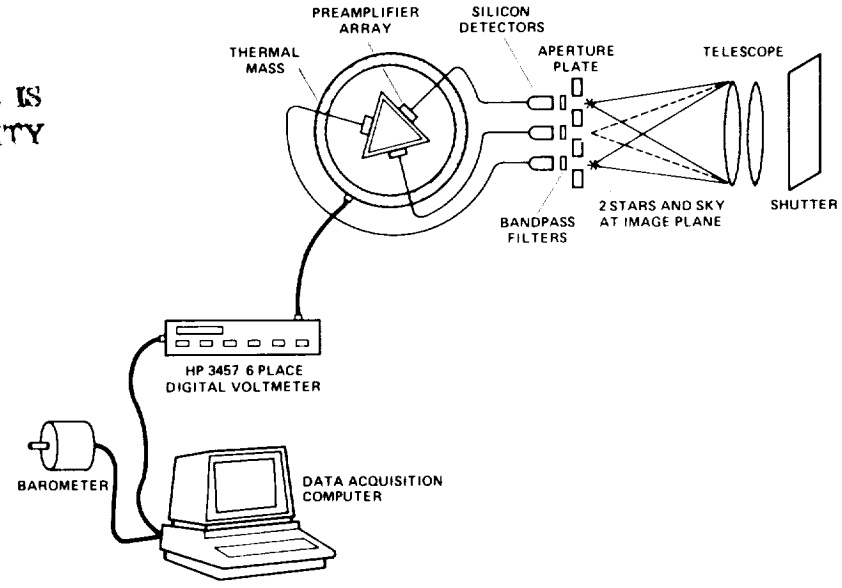

Fig. 1. Schematic diagram of the photometer operation.

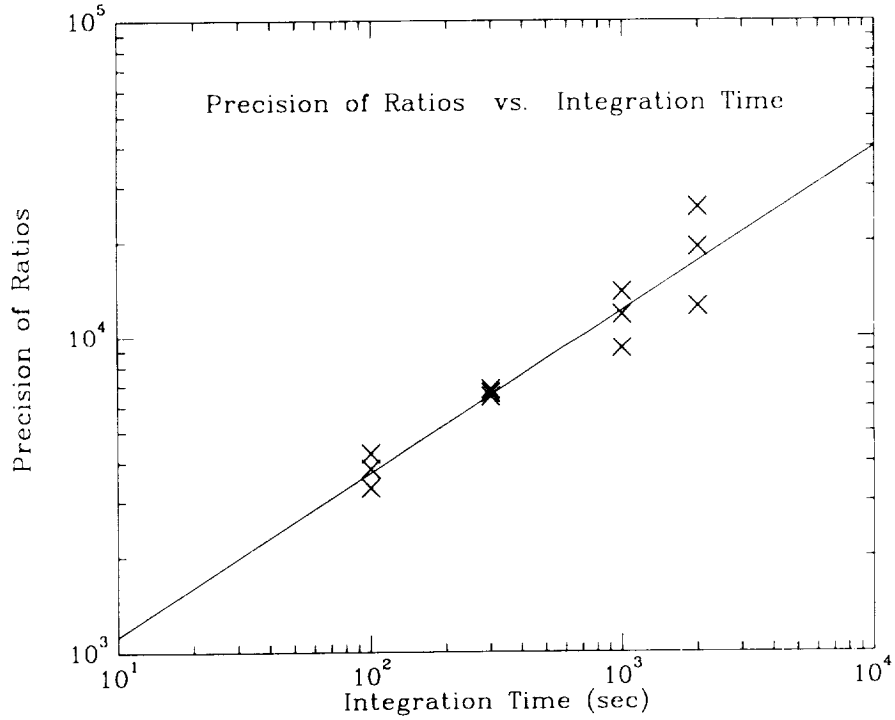

Fig. 2. Laboratory measurements of the precision versus integration time.

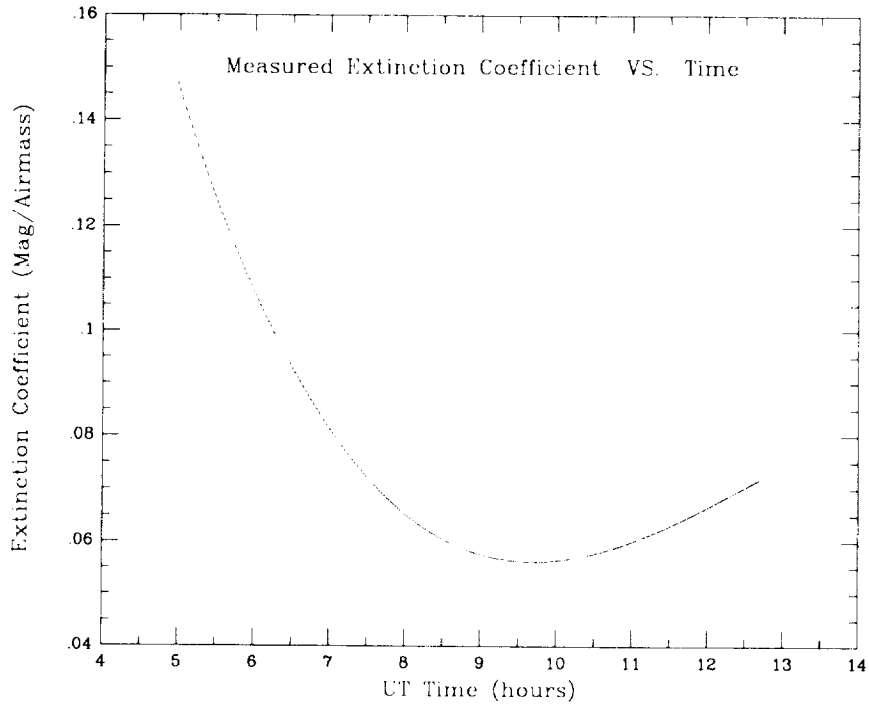

Fig. 3. Measured variation of the extinction coefficient for α ARI versus time on a typical night.

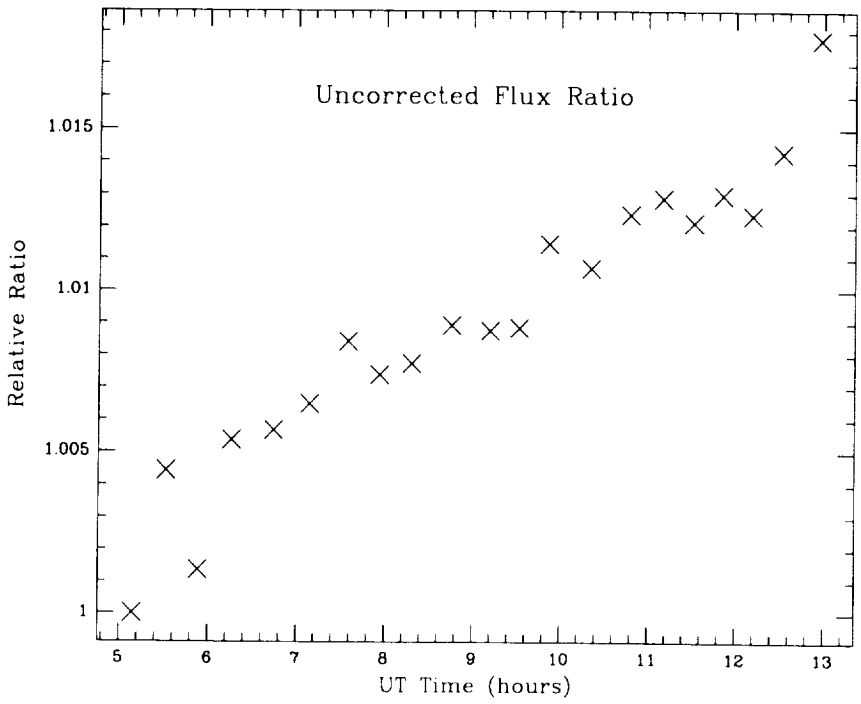

Fig. 4. Measured flux ratio versus time before corrections were made for the time variations of the airmass and extinction coefficients. The ratios are normalized to 1.0 at the first point.

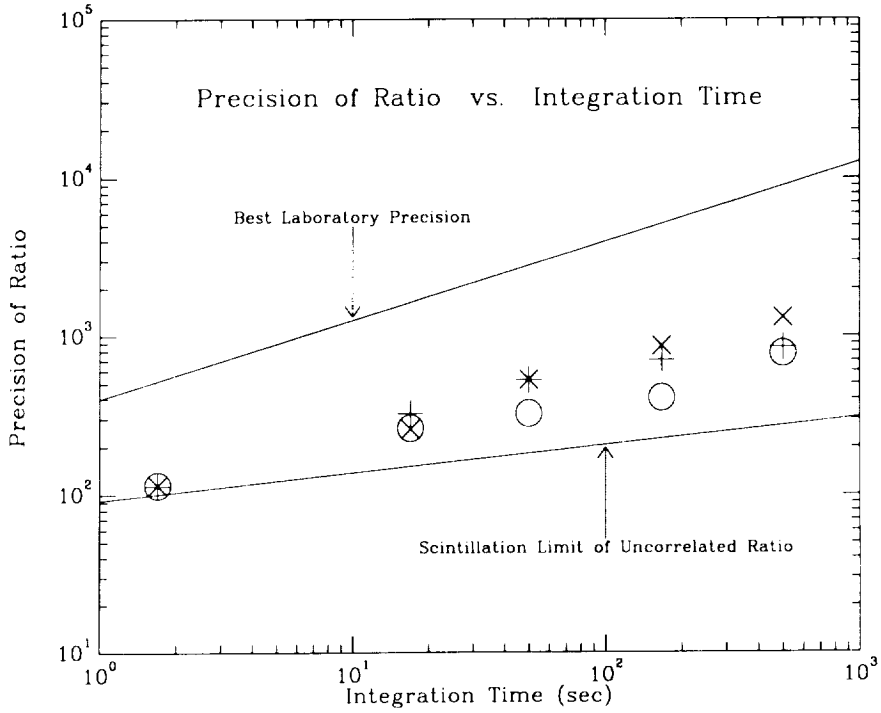

Fig. 5. Measured precision of the flux ratio versus integration time. The symbols represent measurements made at Lick Observatory with the 0.5 m Twin Astrograph. The lower curve represents the scintillation limit predicted from measurements of the individual channels. The upper curve represents the laboratory results.